Acta Crystallographica Section D
Biological Crystallography
ISSN 0907-4449

Away from the edge II: in-house Se-SAS phasing with chromium radiation

Hao Xu,[a]‡ Cheng Yang,[b]‡ Lirong Chen,[a] Irina A. Kataeva,[a] Wolfram Tempel,[a] Doowon Lee,[a] Jeff E. Habel,[a] Duong Nguyen,[a] James W. Pflugrath,[b] Joseph D. Ferrara,[b] W. Bryan Arendall III,[c] Jane S. Richardson,[c] David C. Richardson,[c] Zhi-Jie Liu,[a] M. Gary Newton,[a] John P. Rose[a]* and Bi-Cheng Wang[a]

[a]Southeast Collaboratory for Structural Genomics, Department of Biochemistry and Molecular Biology, The University of Georgia, Athens, GA 30605, USA, [b]Rigaku/Molecular Structure Corporation, The Woodlands, TX 77381, USA, and [c]Department of Biochemistry, Duke University, Durham, NC 27710, USA

‡ These authors contributed equally to this work.

Correspondence e-mail: rose@bcl4.bmb.uga.edu

Received 16 December 2004
Accepted 5 April 2005

PDB Reference: putative chorismate mutase, 1xho, r1xhosf

Recently, the demands of high-throughput macromolecular crystallography have driven continuous improvements in phasing methods, data-collection protocols and many other technologies. Single-wavelength anomalous scattering (SAS) phasing with chromium X-ray radiation opens a new possibility for phasing a protein with data collected in-house and has led to several successful examples of *de novo* structure solution using only weak anomalous scatterers such as sulfur. To further reduce data-collection time and make SAS phasing more robust, it is natural to combine selenomethionine-derivatized protein (SeMet protein) with Cr $K\alpha$ radiation to take advantage of the larger anomalous scattering signal from selenium ($f'' = 2.28\ e^-$) compared with sulfur ($f'' = 1.14\ e^-$). As reported herein, the crystal structure of a putative chorismate mutase from *Clostridium thermocellum* was determined using Se-SAS with Cr $K\alpha$ radiation. Each protein molecule contains eight selenomethionine residues in 148 amino-acid residues, providing a calculated Bijvoet ratio of about 3.5% at the Cr $K\alpha$ wavelength. A single data set to 2.2 Å resolution with approximately ninefold redundancy was collected using an imaging-plate detector coupled with a Cr source. Structure solution, refinement and deposition to the Protein Data Bank were performed within 9 h of the availability of the scaled diffraction data. The procedure used here is applicable to many other proteins and promises to become a routine pathway for in-house high-throughput crystallography.

1. Introduction

Over the past ten years, multiple wavelength anomalous diffraction (MAD; Hendrickson, 1991) in conjunction with synchrotron radiation and selenomethionine-derivatized proteins has been remarkably successful as a method for solving protein structures. Instead of collecting diffraction data on the native crystal and a number of different heavy-atom derivative crystals required for the multiple isomorphous replacement approach (MIR), the MAD technique allows the experimenter to calculate phases from differences in observed intensities brought about by the wavelength-dependent anomalous scattering from certain atoms in the crystal. The traditional MAD approach requires the collection of data sets at three or four different wavelengths around the absorption edge of the anomalous scatterers present in the crystal. Indeed, MAD phasing eliminates the trial-and-error and time-consuming step of the preparation of heavy-atom derivatives. In favorable cases, MAD phases provide experimental electron-density maps of exceptional quality. However, even with the introduction of third-generation synchrotron

sources and many new beamlines in recent years, access to synchrotrons still remains somewhat limited for many research laboratories owing to the increasing demand for synchrotron beam time and the considerable geographical distances to the closest available synchrotron source for many laboratories. We also have seen that two-wavelength (DAD; Hädener *et al.*, 1999; González, 2003), one-and-a-half wavelength (Dauter, 2002) and SAS at peak wavelength (Rice *et al.*, 2000) experiments are growing in popularity, both as a method to use beam time more efficiently and to mitigate the effects of radiation damage. The advantages of these methods have been demonstrated in many successful cases, but they still require a tuneable synchrotron beamline. Therefore, MAD phasing cannot be employed easily in home laboratories. Instead, personnel are required to travel to a synchrotron source and work under unfamiliar experimental conditions.

The emergence of high-throughput structure determination has driven the development of many new methods, ideas and techniques to provide more efficient data collection and more powerful phasing procedures. One of these new techniques is to utilize softer X-rays for phasing protein data (Borek *et al.*, 2002; Chayen *et al.*, 2000; Cianci *et al.*, 2001; Ramagopal *et al.*, 2003; Liu *et al.*, 2000; Stuhrmann *et al.*, 1995; Weiss *et al.*, 2001; Micossi *et al.*, 2002). The first report of the application of Cr $K\alpha$ radiation (λ = 2.29 Å) for phasing dates back to 1958 (Blow, 1958). As a result of various experimental problems such as absorption, low detector sensitivity and low source flux, only a partial and inaccurate data set to low resolution could be recorded. Little progress in phasing using Cr $K\alpha$ radiation was made until high-brilliance Cr sources, cryocrystallography techniques, new detector technologies and more automatic and reliable algorithms became available. All these advances have led to the ability to measure accurately small anomalous intensity differences (∼1–2% of total reflection intensity; Yang *et al.*, 2003). In principle, the relatively long wavelength of Cr $K\alpha$ radiation is well suited for enhancing the signal from weak anomalous scatterers such as S, Se and Ca, as well as other atoms commonly found in proteins, owing to an increased anomalous signal (f'' is 1.14 e^- for S, 2.28 e^- for Se and 2.51 e^- for Ca) at this wavelength compared with the same elements when measured using Cu $K\alpha$ radiation (λ = 1.54 Å; f'' is 0.56 e^- for S, 1.14 e^- for Se and 1.29 e^- for Ca). Several successful examples of Cr sulfur SAS (S-SAS) phasing have been reported recently (Yang *et al.*, 2003; Phillips *et al.*, 2004; Chen *et al.*, 2004; Rose *et al.*, 2004; Madauss *et al.*, 2004). Our previous study (Yang *et al.*, 2003) on crystals of thaumatin and trypsin demonstrated enhancement of the anomalous signal using Cr $K\alpha$ radiation. One benefit of using longer wavelengths is that less data were needed for phasing compared with data collected using Cu $K\alpha$ radiation (Yang & Pflugrath, 2001; Debreczeni *et al.*, 2003; Lemke *et al.*, 2002; Stevenson *et al.*, 2004; Olsen *et al.*, 2004). Indeed, the recent successes of Cr S-SAS phasing provide an alternative method for crystallographers experiencing difficulty with heavy-atom incorporation and/or with access to a synchrotron source. However, Wang (1985), who studied simulations based on the anomalous scattering of two S atoms in the 12 kDa Rhe native protein, concluded that a successful structure solution by S-SAS phasing would require a Bijvoet ratio ($\langle|\Delta F|\rangle/\langle F\rangle$) of at least 0.6%. Thus, the signal-to-noise ratio of the data is also critical for success.

Over the past few years, many methods have been developed to incorporate additional anomalous scatterers into protein molecules for phasing. These methods include short cryosoaking with the halides Br^- and I^- (Dauter *et al.*, 2000; Usón *et al.*, 2003), the use of positively and negatively charged counterions Gd^{3+}, Cs^+, I^- and Cl^- (Evans & Bricogne, 2002; Nagem *et al.*, 2001), the use of triiodide $[I_3]^-$ (Evans & Bricogne, 2002), Xe derivatization under pressure (Sauer *et al.*, 1997; Djinovic Carugo *et al.*, 1998; Schubot *et al.*, 2001), a combination of halides and Xe (Panjikar & Tucker, 2002) and short soaks with traditional heavy-atom compounds (Sun *et al.*, 2002). The newly reported site-specific incorporation of *p*-iodo-L-phenylalanine provides another way to selectively introduce heavy-atom-containing amino acids into protein (Xie *et al.*, 2004). In addition, this incorporation allows control of the number of I atoms incorporated and location of I atoms by genetically encoding iodoPhe with a unique codon. Successful incorporation of these elements increases the possibility of success, especially for SAS phasing (Chen *et al.*, 1991), making the process more robust and reducing data-collection time. Currently, the most popular approach of incorporating a heavy atom is production of selenomethionine protein by replacing methionine with selenomethionine, especially in *Escherichia coli* (Hendrickson *et al.*, 1990). Some examples of Se incorporation *via* insect and mammalian cells (Bellizzi *et al.*, 1999; McWhirter *et al.*, 1999; Lustbader *et al.*, 1995) have also been reported. This technology, together with cryocrystallography and synchrotron beamlines, are three essential components for MAD phasing and are partially responsible for the evolution of macromolecular crystallography to the point that high-throughput structure-determination pipelines, aimed at solving new structures at an unprecedented pace, have been developed in many laboratories. Currently, selenomethionine derivatization has become a simple and routine tool used in almost every crystallography laboratory.

It has been reported previously that the anomalous signal from selenomethionine can be accurately measured on an in-house Cu source (Jaskólski & Wlodawer, 1996; Lemke *et al.*, 2002). Using an in-house X-ray source, the anomalous scattering strength of selenium (f'' = 1.14 e^-) is twice that of sulfur (f'' = 0.56 e^-) when measured using Cu $K\alpha$ X-rays and is doubled again (f'' = 2.28 e^-) if Cr $K\alpha$ radiation is used. This suggests that the combination of Cr $K\alpha$ radiation and selenomethionine-derivatized protein may prove to be a powerful tool in carrying out high-throughput *de novo* structure determination in the home laboratory. However, given the fact that at its K absorption edge f'' values for selenium range between 3.7 and 6.6 e^-, it is evident that the anomalous scattering signal of selenium is stronger when collected at its K absorption edge using synchrotron radiation. However, when availability of X-rays, transportation of personnel and crystals, and familiarity of working environment are considered, an

in-house Cr source may be a very useful alternative to a synchrotron beamline.

This paper reports the crystal structure of chorismate mutase from *Clostridium thermocellum* (Cth-682) determined using selenium SAS (Se-SAS) data measured with Cr $K\alpha$ radiation. Chorismate mutase has three monomers in the asymmetric unit, with each monomer containing 148 residues, including eight selenomethionine residues. The calculated Bijvoet ratio for the trimer in the asymmetric unit is ~3.5% for Cr $K\alpha$, which is almost six times the minimum ratio found by the S-SAS simulation of Wang (1985).

2. Materials and methods

Highly pure Cth-682 protein was prepared by the SECSG Crystallomics Group using published procedures (Wang *et al.*, 2005) as outlined in the supplementary material.[1] Protein purity was assayed using SDS–PAGE and concentrated to 55 mg ml^{-1} (based on extinction at 280 nm wavelength).

The protein was crystallized by the sitting-drop vapour-diffusion method. Using a Crystalquick plate (square wells, Greiner Bio-One), 200 nl protein solution was mixed with an equal volume of crystallization reagent that consisted of aqueous 2.5 *M* ammonium sulfate and 100 m*M* HEPES pH 7.6. The resulting drop was equilibrated against 150 µl crystallization reagent. After setup, the plate was sealed with CrystalSeal film (Hampton Research) and incubated for five weeks at 291 K.

For data collection, a crystal was briefly immersed into a 4:1 mixture of crystallization reagent and glycerol, and flash-frozen in a cryoloop (Teng, 1990; Hampton Research) by immersion into liquid nitrogen.

X-rays were generated with a chromium target on an RU-H3R generator and focused through Cr CMF optics (Osmic). A data set consisting of a single-axis φ scan with 720 half-degree oscillation images was recorded under cooling (Hope, 1988) on a modified R-AXIS IV detector (Rigaku) using a crystal-to-detector distance of 96 mm and an exposure time of 240 s per image. The total data-collection time was approximately 48 h. The modifications to the R-AXIS detector included a helium-flushed diffracted beam path to reduce air absorption and a modified beam stop described elsewhere (Yang *et al.*, 2003).

The structure determination was carried out as follows. Firstly, data reduction was carried out using the *HKL*2000 suite (Otwinowski & Minor, 1997). The scaled structure factors were then used together with an automated structure-determination pipeline, *SCA2STRUCTURE* (Liu *et al.*, 2005), to solve the structure in under 4 h. Therein, the structure was phased using the programs *SOLVE* and *RESOLVE* (Terwilliger, 2004). The solvent content used in the calculations was estimated to be 43%. The entire structure was automatically traced by the program *ARP*/*wARP* (Perrakis *et al.*, 2001).

[1] Supplementary material has been deposited in the IUCr electronic archive (Reference: EA5036). Services for accessing these data are described at the back of the journal.

Table 1
Data-reduction results.

Values in parentheses are for the last resolution shell.

Wavelength (Å)	2.29
XG power (kW)	4.5
Space group	$P3_1$
Unit-cell parameters (Å)	a = 48.20, b = 48.20, c = 123.69
Mosacity (°)	0.6–0.7
Resolution (Å)	10.00–2.20 (2.28–2.20)
$R(I)_{\rm merge}$ (%)	5.7 (16.7)
Unique reflections	15073 (688)
Completeness (%)	93.3 (42.6)
Redundancy	9.7 (2.3)
$\langle I/\sigma(I)\rangle$	43.0 (4.5)

For cross-validation, free reflections were selected in thin resolution shells with the program *DATAMAN* (Kleywegt & Brünger, 1996; Kleywegt, 1996). The model was iteratively refined, validated and rebuilt in several cycles using the programs *REFMAC* (Murshudov, 1997), *MOLPROBITY* (Lovell *et al.*, 2003; Davis *et al.*, 2004) and *XFIT* (McRee, 1999), respectively. No non-crystallographic symmetry restraints were used in the refinement. Further validation with *PROCHECK* (Laskowski *et al.*, 1993) was performed prior to deposition (*PDB_EXTRACT*; Yang *et al.*, 2004) of the model coordinates and structure-factor amplitudes in the Protein Data Bank (Berman *et al.*, 2000; entry 1xho).

3. Results and discussion

The Cth-682 gene encodes 118 amino-acid residues, of which seven are selenomethionine and two are cysteine. A tag of 30 residues was prefixed to the Cth-682 sequence during cloning to facilitate protein expression and purification and included one additional selenomethionine. This protein, with a length of 148 residues, was used in crystallization without cleavage of the prefixed sequence.

A single crystal of Cth-682 was harvested from the crystallization drop, cryoprotected, flash-cooled in liquid nitrogen and mounted in an arbitrary orientation on the goniometer while being maintained at 100 K in a nitrogen-gas cryostream. Data were collected under cryogenic conditions with a single 360° φ scan within approximately 48 h and no special data-collection scheme was employed. In order to obtain an accurate anomalous signal, a data set of approximately tenfold redundancy was collected to a resolution of 2.2 Å. The data-collection and processing statistics are listed in Table 1. A sharp drop in data completeness is observed beyond 2.4 Å resolution (Table 2) and can be attributed to the data recorded from the corners of the imaging plate where the resolution extends to 2.20 Å. In total, 552 843 observations were used in data processing and 3342 (0.61%) were rejected.

With respect to the strength of the anomalous signal, introduction of selenium through incorporation of selenomethionine into the polypeptide confers two distinct advantages: (i) successful derivatization is more likely and (ii) the resulting selenium occupancies are higher than those of traditional heavy-atom derivatives prepared by a trial-and-

Table 2
Data completeness by resolution shell.

Resolution (Å)	Completeness (%)	R_{sym}† (%)
10.00–4.60	99.7	5.2
4.60–3.71	100.0	4.6
3.71–3.26	100.0	5.2
3.26–2.97	100.0	5.9
2.97–2.76	100.0	7.2
2.76–2.60	100.0	9.3
2.60–2.47	100.0	11.8
2.47–2.37	99.9	15.7
2.37–2.28	89.7	16.2
2.28–2.20	42.9	16.7

† $R_{sym} = \sum |I - \bar{I}| / \sum I$.

error soaking approach (Doublié, 1997). In addition, the selenium positions can serve as guides during the model-building process, which can facilitate the fitting process significantly.

Since Cth-682 contains two types of anomalous scatterers (Se and S) and the ratios of their f'' values are ∼2 at both the Cu $K\alpha$ and Cr $K\alpha$ wavelengths, the contribution from S atoms to the overall scattering is significant. Therefore, the formalism of Hendrickson & Teeter (1981) may not be sufficient to estimate the Bijvoet ratio ($\Delta_{ano} = \langle|\Delta F|\rangle/\langle F\rangle$). We have adopted the formalism presented by Olczak *et al.* (2003) to calculate Δ_{ano}, which consists of not only individual contributions Δ^{Se}_{ano} and Δ^{S}_{ano} arising from the scatterers Se and S but also contains a mixed term $\Delta_{ano} = [(\Delta^{Se}_{ano})^2 + (\Delta^{S}_{ano})^2 + (\Delta^{SeS}_{ano})^2]^{1/2}$.

The results of these calculations are summarized in Table 3. The table shows that the overall calculated Bijvoet ratio increases by 100% by simply changing radiation from Cu $K\alpha$ (λ = 1.54 Å) to Cr $K\alpha$ (λ = 2.29 Å). Furthermore, by replacing methionine with selenomethionine in the crystal and using Cr $K\alpha$ radiation, the Bijvoet ratio increases 3.7-fold compared with that using a native crystal with Cu $K\alpha$ radiation. These values strongly suggest that combining Se-derivatized protein and Cr $K\alpha$ radiation would be beneficial to in-house SAS phasing. The experimental value of the Bijvoet ratio, Δ_{ano} = 5%, is larger than the theoretical value. This is a result of approximations in Olczak's formula (see, for example, Shen *et al.*, 2003), systematic errors such as absorption, and random errors in the measured intensities. The overall anomalous signal from selenomethionyl Cth-682 is dominated by the Se atoms; however, the anomalous signal of the remaining S atoms is not negligible since it is estimated to be a quarter of the total anomalous signal produced by the Se atoms. This has been demonstrated by the fact that three S atoms were located among 15 Se atoms found by *SOLVE*, giving the 18 sites listed in Table 4. The refined temperature factors for the three unobserved Se atoms [residues Mse64(*A*), Mse72(*A*) and Mse72(*B*)] were 56, 54 and 49 Å^2, respectively, and were higher than the mean temperature factor for all refined atoms (29.8 Å^2). The Se atoms of Mse64(*C*) and Mse72(*C*) with high temperature factors (>50 Å^2) were located by *SOLVE*, but their peak heights are close to and lower than the three found S atoms, which had an average temperature factor of 24 Å^2.

Table 3
Wavelength-dependent contributions of selenium and sulfur anomalous scatterers in crystals of Cth-682.

X-ray source	Cu $K\alpha$		Cr $K\alpha$	
Protein	Native	SeMet	Native	SeMet
f'_S	0.319	0.319	0.374	0.374
f''_S	0.557	0.557	1.142	1.142
f'_{Se}		−0.879		−0.273
f''_{Se}		1.139		2.283
Δ^{S}_{ano} (%)	0.9	0.4	1.8	0.8
Δ^{Se}_{ano} (%)		1.5		3.1
Δ^{SeS}_{ano} (%)		0.3		0.6
Δ_{ano}(calc) (%)	0.9	1.6	1.8	3.3
Δ_{ano}(obs) (%)				5.0
$\langle\Delta F\rangle/\langle\sigma(\Delta F)\rangle$ (obs) (%)				1.2

Table 4
Peak heights (*SOLVE*) and assignments of anomalous scatterers used in the structure solution of Cth-682.

Refined isotropic temperature factors for SE (selenomethionine) and SG atoms (cysteine) from *REFMAC* are also shown.

Position	Peak height (σ)	Residue	Chain	*B* factor (Å^2)
1	12.9	Mse30	*A*	30.0
2	12.2	Mse64	*B*	37.1
3	12.1	Mse90	*A*	33.0
4	11.6	Mse30	*B*	29.6
5	11.2	Mse90	*C*	30.4
6	10.4	Mse30	*C*	30.8
7	10.2	Mse91	*C*	32.6
8	10.0	Mse91	*A*	37.6
9	9.71	Mse91	*B*	34.0
10	9.49	Mse74	*A*	40.3
11	9.45	Mse90	*B*	34.1
12	8.95	Mse74	*B*	36.7
13	8.85	Mse74	*C*	35.9
14	7.40	Mse64	*C*	53.8
15	7.14	Cys73	*A*	24.3
16	6.58	Cys73	*C*	24.8
17	6.52	Cys86	*C*	23.7
18	5.99	Mse72	*B*	56.8

This indicates that the multiple conformations observed for these side chains in the crystal indeed reduce the anomalous signal contribution from these Se atoms. The Se atom of residue Mse1 has not been modelled for any of the three chains. It is also noteworthy that the detected S atoms belong to 'standalone' cysteinyl residues as opposed to 'superatoms' in disulfide bridges.

The 18 positions from *SOLVE* were treated as Se atoms for phase calculation and refinement. A total of 14 517 anomalous differences up to a resolution of 2.2 Å were used at this stage. The initial figure of merit from *SOLVE* was 0.39, which is lower than what one would expect from MAD phasing. However, this is understandable since anomalous scattering data collected at a single wavelength cannot produce unimodal phase-probability distributions. It is essential to apply density-modification techniques, especially solvent flattening, to resolve the SAS phase ambiguity (Wang, 1985). In addition, *RESOLVE*'s analysis of the substructure solution permitted the determination of threefold non-crystallographic symmetry transformations and subsequent density averaging. The figure of merit was increased to 0.54 after density-modification

procedures. This resulted in an experimental electron-density map of very high quality. The map correlation coefficient reaches 0.89 and 0.87 for atoms of the main chain and side chains, respectively, when referred to a σ_A-weighted $2F_o - F_c$ electron-density map computed from the refined model. The quality of the electron-density map after density modification is shown in Fig. 1. These phases, combined with experimental data extending to 2.2 Å resolution, facilitated automated building of a partially refined model. Further refinement and validation resulted in a crystallographic R factor of 19.4% (R_{free} = 25.5%; Table 5). It is noteworthy that starting from processed diffraction data, PDB deposition of the refined model could be accomplished on the same working day.

Cth-682 consists of two α-helices and a four-stranded β-sheet (Fig. 2*a*). The peptide forms a trimer, which comprises the crystallographic asymmetric unit. The individual molecules are related by a non-crystallographic threefold axis. Each monomer contributes four β-strands to form a β-barrel (Fig. 2*b*). Hydrophobic residues Ile45, Val2 and the charged side chains of His92 from all three monomers are observed in the centre of the barrel. Three selenomethionine (Mse72, Mse74 and Mse90) residues of each protein molecule are also located nearby. This predominantly hydrophobic core is assumed to stabilize the configuration of the trimer. Since Cth-682 is a structural genomics target, it has yet not been subjected to experiments to elucidate the potential biochemical significance of the oligomeric state. The N-terminal cloning/purification tag was not observed in the electron-density maps and theses residues were assumed to be disordered.

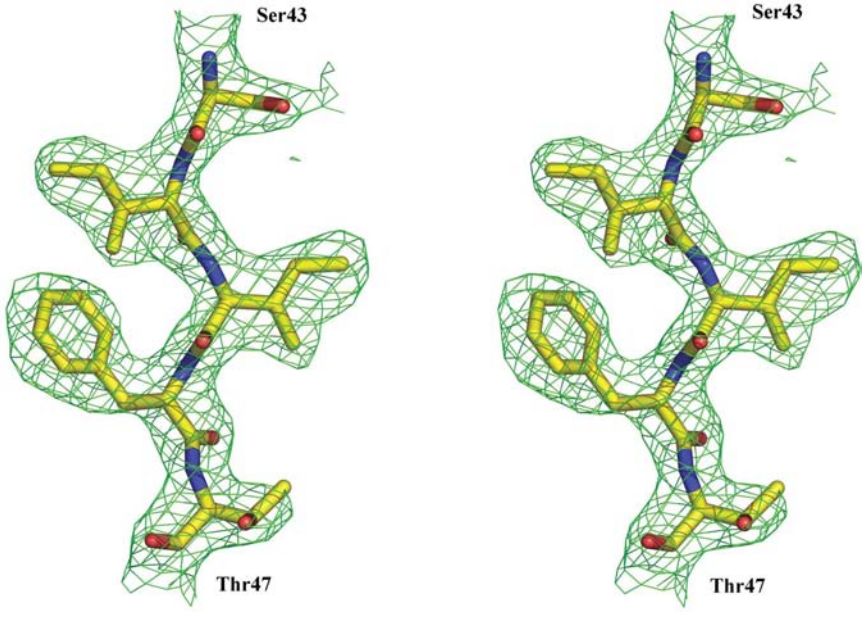

Figure 1
A stereoview of a section of the experimental electron-density map of the chorismate mutase structure generated from data to 2.2 Å resolution from Se/S-SAS phases derived from Cr $K\alpha$ data. The map is contoured at 1σ. The figure was generated with *PyMOL* (DeLano, 2002). The electron-density map was generated by using the phases after the density-modification procedure in *RESOLVE*.

Table 5
Model statistics.

Values in parentheses are for the highest resolution shell.

Resolution (Å)	10.00–2.20 (2.25–2.20)
R/R_{free} (%)	19.4/25.5 (29.8/†)
R.m.s.d. from ideal	
Bond lengths (Å)	0.012
Angles (°)	1.1
Non-H atoms refined	2634
Mean B value/Wilson B value (Å^2)	29.8/38.9

† Owing to low completeness in this shell and owing to the 'thin shell' selection method, no reflections were flagged for cross-validation.

4. Conclusions

Numerous examples reported in the last few years demonstrate that the SAS approach is fully capable of solving the phase problem in protein crystallography. The recent success of S-SAS phasing using Cr $K\alpha$ radiation reveals the possibilities for S-SAS phasing in the home laboratory. However, as in other approaches, the success of S-SAS in previous examples does not guarantee success in all cases, since S-SAS phasing success hinges on the quality of the sample and the signal-to-noise level of the data. Thus, Se-SAS using chromium X-rays offers an attractive means of increasing the success rate of in-house SAS phasing, since selenium provides twice the anomalous scattering signal compared with that of sulfur for both Cu $K\alpha$ and Cr $K\alpha$ X-radiation. In addition, since selenomethionine labelling of proteins for crystal structure-determination purposes has become a routine tool of structural biologists, in-house Se-SAS structure determination using Cr X-rays offers a convenient and readily available alternative to MAD/SAS structure determination at a synchrotron.

The selenium-SAS experiment described here made use of a conventional Rigaku RU-H3R rotating-anode generator with a chromium anode, a set of first-generation chromium confocal optics and a Rigaku R-AXIS IV imaging-plate detector modified by placing a helium beam path between the crystal and the detector. The data-collection strategy consisted of a simple 360° rotation of the crystal in the X-ray beam with data recorded every half degree. This strategy has proven effective in numerous S-SAS structure determinations (see Rose *et al.*, 2004). Data processing was straightforward using *HKL*2000 and no special treatment of the data was applied during processing or scaling. The fact that a refined structure could be automatically determined from one set of Se-SAS data also attests to the power of this approach.

The average frequency of sulfur-containing amino acids in 24 bacterial proteomes has been estimated as 1.1% for

cysteine and 2.2% for methionine (Jauregui *et al.*, 2000), providing about 3.3 S atoms per 100 amino acids on average. Based on this estimate, the average protein would have a Bijvoet ratio of 1.5% when using Cr $K\alpha$ radiation, which is above the 0.6% value used by Wang in his simulations on Bence–Jones protein Rhe (Furey *et al.*, 1983). When selenomethionine protein is used, the Bijvoet ratio for the average protein is increased to 2.6%, which may enable Se-SAS phasing using Cr X-rays to become a routine tool for rapid in-house structure determination as illustrated in the work reported here.

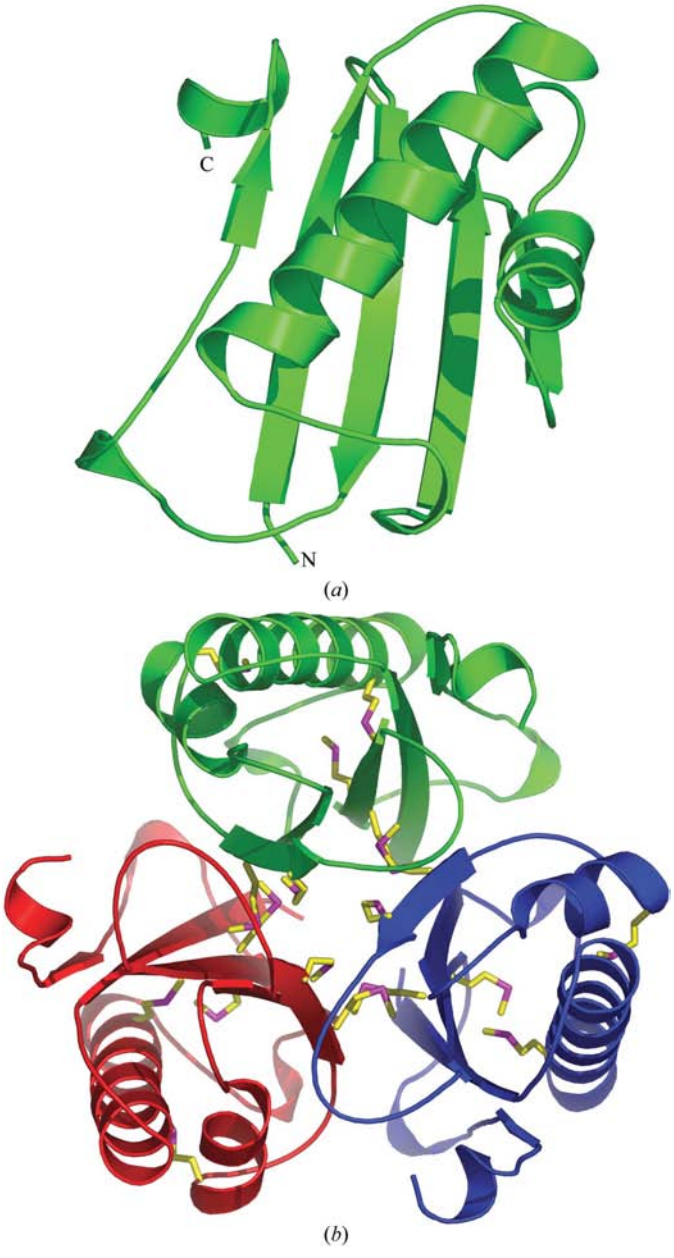

Figure 2
Ribbon diagrams of the Cth-682 model: (*a*) monomer and (*b*) the trimer constituting the asymmetric unit. The side chains of selenomethionine residues are shown in stick mode.

Financial support from the National Institutes of Health (GM62407 and 60329), IBM Life Sciences, the Georgia Research Alliance and the University of Georgia Research Foundation is acknowledged. The authors thank Professor Ming Luo, The University of Alabama at Birmingham for vectors used in cloning of Cth-682.

References

Bellizzi, J. J., Widom, J., Kemp, C. W. & Clardy, J. (1999). *Structure Fold. Des.* **7**, R263–R267.
Berman, H. M., Westbrook, J., Feng, Z., Gilliland, G., Bhat, T. N., Weissig, H., Shindyalov, I. N. & Bourne, P. E. (2000). *Nucleic Acids Res.* **28**, 235–242.
Blow, D. M. (1958). *Proc. R. Soc. London Ser. A*, **247**, 302–336.
Borek, D., Minor, W. & Otwinowski, Z. (2002). Abstr. Am. Crystallogr. Assoc. Annu. Meet., Abstract P024.
Chayen, N. E., Cianci, M., Olczak, A., Raftery, J., Rizkallah, P. J., Zagalsky, P. F. & Helliwell, J. R. (2000). *Acta Cryst.* D**56**, 1064–1066.
Chen, L., Chen, L. R., Zhou, X. E., Wang, Y., Kahsai, M. A., Clark, A. T., Edmondson, S. P., Liu, Z. J., Rose, J. P., Wang, B.-C., Meehan, E. J. & Shriver, J. W. (2004). *J. Mol. Biol.* **341**, 73–91.
Chen, L. Q., Rose, J. P., Breslow, E., Yang, D., Chang, W. R., Furey, W. F. Jr, Sax, M. & Wang, B.-C. (1991). *Proc. Natl Acad. Sci. USA*, **88**, 4240–4244.
Cianci, M., Rizkallah, P. J., Olczak, A., Raftery, J., Chayen, N. E., Zagalsky, P. F. & Helliwell, J. R. (2001). *Acta Cryst.* D**57**, 1219–1229.
Dauter, Z. (2002). *Acta Cryst.* D**58**, 1958–1967.
Dauter, Z., Dauter, M. & Rajashankar, K. R. (2000). *Acta Cryst.* D**56**, 232–237.
Davis, I. W., Murray, L. W., Richardson, J. S. & Richardson, D. C. (2004). *Nucleic Acids Res.* **32**, W615–W619.
Debreczeni, J. É., Bunkoczi, G., Ma, Q., Blaser, H. & Sheldrick, G. M. (2003). *Acta Cryst.* D**59**, 688–696.
DeLano, W. L. (2002). *PyMOL.* DeLano Scientific, San Carlos, CA, USA.
Djinovic Carugo, K., Everitt, P. & Tucker, P. A. (1998). *J. Appl. Cryst.* **31**, 812–814.
Doublié, S. (1997). *Methods Enzymol.* **276**, 523–530.
Evans, G. & Bricogne, G. (2002). *Acta Cryst.* D**58**, 976–991.
Furey, W. Jr, Wang, B.-C., Yoo, C. S. & Sax, M. (1983). *J. Mol. Biol.* **167**, 661–692.
González, A. (2003). *Acta Cryst.* D**59**, 315–322.
Hädener, A., Matzinger, P. K., Battersby, A. R., McSweeney, S., Thompson, A. W., Hammersley, A. P., Harrop, S. J., Cassetta, A., Deacon, A., Hunter, W. N., Nieh, Y. P., Raftery, J., Hunter, N. & Helliwell, J. R. (1999). *Acta Cryst.* D**55**, 631–643.
Hendrickson, W. A. (1991). *Science*, **254**, 51–58.
Hendrickson, W. A., Horton, J. R. & LeMaster, D. M. (1990). *EMBO J.* **9**, 1665–1672.
Hendrickson, W. A. & Teeter, M. M. (1981). *Nature (London)*, **290**, 107–113.
Hope, H. (1988). *Acta Cryst.* B**44**, 22–26.
Jaskólski, M. & Wlodawer, A. (1996). *Acta Cryst.* D**52**, 1075–1081.
Jauregui, R., Bolivar, F. & Merino, E. (2000). *Microb. Comput. Genomics*, **5**, 7–15.
Kleywegt, G. J. (1996). *Acta Cryst.* D**52**, 826–828.
Kleywegt, G. J. & Brünger, A. T. (1996). *Structure*, **4**, 897–904.
Laskowski, B. A., MacArthur, M. W., Moss, D. S. & Thornton, J. M. (1993). *J. Appl. Cryst.* **26**, 283–291.
Lemke, C. T., Smith, G. D. & Howell, P. L. (2002). *Acta Cryst.* D**58**, 2096–2101.
Liu, Z.-J., Lin, D., Tempel, W., Praissman, J., Rose, J. P. & Wang, B.-C. (2005). *Acta Cryst.* D**61**, 520–527.
Liu, Z.-J., Vysotski, E. S., Chen, C. J., Rose, J. P., Lee, J. & Wang, B.-C. (2000). *Protein Sci.* **9**, 2085–2093.

Lovell, S. C., Davis, I. W., Arendall, W. B., de Bakker, P. I., Word, J. M., Prisant, M. G., Richardson, J. S. & Richardson, D. C. (2003). *Proteins*, **50**, 437–450.
Lustbader, J. W., Wu, H., Birken, S., Pollak, S., Kolks, M. A. G., Pound, A. M., Austen, D., Hendrickson, W. A. & Canfield, R. E. (1995). *Endocrinology*, **136**, 640–650.
McRee, D. E. (1999). *J. Struct. Biol.* **125**, 156–165.
McWhirter, S. M., Pullen, S. S., Holton, J. M., Crute, J. J., Kehry, M. R. & Alber, T. (1999). *Proc. Natl Acad. Sci. USA*, **96**, 8408–8413.
Madauss, K., Juzumiene, D., Waitt, G., Williams, J. & Williams, S. (2004). *Endocr. Res.* **30**, 775–785.
Micossi, E., Hunter, W. N. & Leonard, G. A. (2002). *Acta Cryst.* D**58**, 21–28.
Murshudov, G. N. (1997). *Acta Cryst.* D**53**, 240–255.
Nagem, R. A., Dauter, Z. & Polikarpov, I. (2001). *Acta Cryst.* D**57**, 996–1002.
Olczak, A., Cianci, M., Hao, Q., Rizkallah, P. J., Raftery, J. & Helliwell, J. R. (2003). *Acta Cryst.* A**59**, 327–334.
Olsen, J. G., Flensburg, C., Olsen, O., Bricogne, G. & Henriksen, A. (2004). *Acta Cryst.* D**60**, 250–255.
Otwinowski, Z. & Minor, W. (1997). *Methods Enzymol.* **276**, 307–326.
Panjikar, S. & Tucker, P. A. (2002). *Acta Cryst.* D**58**, 1413–1420.
Perrakis, A., Harkiolaki, M., Wilson, K. S. & Lamzin, V. S. (2001). *Acta Cryst.* D**57**, 1445–1450.
Phillips, J. D., Whitby, F. G., Warby, C. A., Labbe, P., Yang, C., Pflugrath, J. W., Ferrara, J. D., Robinson, H., Kushner, J. P. & Hill, C. P. (2004). *J. Biol. Chem.* **279**, 38960–38968.
Ramagopal, U. A., Dauter, M. & Dauter, Z. (2003). *Acta Cryst.* D**59**, 1020–1027.
Rice, L. M., Earnest, T. N. & Brunger, A. T. (2000). *Acta Cryst.* D**56**, 1413–1420.
Rose, J. P., Liu, Z. J., Tempel, W., Chen, D., Lee, D., Newton, M. G. & Wang, B.-C. (2004). *Rigaku J.* **21**, 1–9.
Sauer, O., Schmidt, A. & Kratky, C. (1997). *J. Appl. Cryst.* **30**, 476–486.
Schubot, F. D., Chen, C. J., Rose, J. P., Dailey, T. A., Dailey, H. A. & Wang, B.-C. (2001). *Protein Sci.* **10**, 1980–1988.
Shen, Q., Wang, J. & Ealick, S. E. (2003). *Acta Cryst.* A**59**, 371–373.
Stevenson, C. E., Tanner, A., Bowater, L., Bornemann, S. & Lawson, D. M. (2004). *Acta Cryst.* D**60**, 2403–2406.
Stuhrmann, S., Hutsch, M., Trame, C., Thomas, J. & Stuhrmann, H. B. (1995). *J. Synchrotron Rad.* **2**, 83–86.
Sun, P. D., Radaev, S. & Kattah, M. (2002). *Acta Cryst.* D**58**, 1092–1098.
Teng, T.-Y. (1990). *J. Appl. Cryst.* **23**, 387–391.
Terwilliger, T. (2004). *J. Synchrotron Rad.* **11**, 49–52.
Usón, I., Schmidt, B., von Bulow, R., Grimme, S., von Figura, K., Dauter, M., Rajashankar, K. R., Dauter, Z. & Sheldrick, G. M. (2003). *Acta Cryst.* D**59**, 57–66.
Wang, B.-C. (1985). *Methods Enzymol.* **115**, 90–112.
Wang, B.-C. *et al.* (2005). In the press.
Weiss, M. S., Sicker, T., Djinovic Carugo, K. & Hilgenfeld, R. (2001). *Acta Cryst.* D**57**, 689–695.
Xie, J., Wang, L., Wu, N., Brock, A., Spraggon, G. & Schultz, P. G. (2004). *Nature Biotechnol.* **22**, 1297–1301.
Yang, C. & Pflugrath, J. W. (2001). *Acta Cryst.* D**57**, 1480–1490.
Yang, C., Pflugrath, J. W., Courville, D. A., Stence, C. N. & Ferrara, J. D. (2003). *Acta Cryst.* D**59**, 1943–1957.
Yang, H., Guranovic, V., Dutta, S., Feng, Z., Berman, H. M. & Westbrook, J. D. (2004). *Acta Cryst.* D**60**, 1833–1839.